Supporting Online Material for

Formation of Box Canyon, Idaho, by Megaflood: Implications for Seepage Erosion on Earth and Mars

Michael P. Lamb,* William E. Dietrich, Sarah M. Aciego, Donald J. DePaolo, Michael Manga

*To whom correspondence should be addressed. E-mail: mpl@berkeley.edu

Published 23 May 2008, *Science* **320**, 1067 (2008)
DOI: 10.1126/science.1156630

This PDF file includes:

Supporting Online Materials for:

Formation of Box Canyon Idaho by Megaflood: Implications for Seepage Erosion on Earth and Mars

Michael P. Lamb*, William E. Dietrich, Sarah M. Aciego, Donald J. DePaolo, Michael Manga

University of California, Department of Earth and Planetary Science
Berkeley, CA, 94720-4768

*mpl@berkeley.edu

This PDF file includes:
Materials and Methods
SOM Text
Figs. S1 to S6
Table S1
References and Notes

Materials and Methods

Discharge at incipient motion

We estimated the flow needed to carve Box Canyon from the dimensionless bed-shear stress or Shields stress at incipient sediment motion τ_{*c}:

$$\tau_{*c} = \frac{\tau_b}{(\rho_s - \rho) g D_{50}} \qquad (1)$$

where τ_b is the bed shear-stress, ρ_s and ρ are the densities of sediment and fluid, respectively, g is the acceleration due to gravity, and D_{50} is the median grain diameter

(*S1, S2*). We assume steady and uniform flow, i.e. $\tau_b = \rho g R S$, where R is the hydraulic radius and S is the water-surface slope.

To evaluate equation (1), we made measurements within a 125-m reach (Fig. S1A) along the canyon floor (marked "Measurement Reach" in Fig. 3), which was chosen because it was relatively straight in planform and wadeable. The bed is bouldery throughout the canyon and is probably best described as plane-bed morphology (*S3*), although there are local clusters of boulders and pools. The grain size distribution was measured within this reach (Fig. S2) and the particle-size statistics are D_{84} = 0.60 m, D_{50} = 0.29 m, and D_{16} = 0.13 m, where the subscripts denote the percentage of grains finer than. We measured the intermediate axes of 100 grains by counting particles every 1 m along the channel and conducting four transects spaced ~10 m apart (Fig. S1A). Owing to the large size of particles, measurements were made *in situ* using a tape measure and snorkel gear. A few grains were larger than 1 m across and these were counted twice in the distribution. The particle sizes were binned following the phi scale.

The longitudinal profile of the water surface was measured from 1-m resolution airborne Light Detection and Ranging (LiDAR) data collected by the National Center for Airborne Laser Mapping (Fig. S3). The profile was extracted from a digital elevation model (DEM) following the path of steepest descent, and this profile was verified to be accurate by comparison with a field survey within the measurement reach conducted with a self-leveling level and stadia rod. During floods, bed irregularities will be drowned out and the water surface-slope will tend to be more uniform over a length scale of many times the channel width. To account for this, we estimated the water-surface slope during flood as the average water-surface slope over a 900-m reach bounded by the waterfall

downstream and the canyon headwall upstream (Profile P2, Fig. S3). Using a linear least-squares fit, the slope was found to be S = 1.85%, and for this channel slope τ_{*_c} = 0.055 (*S4*). Using these values, the necessary bed shear-stress to move the bouldery bed was calculated from equation (1) to be 290 N/m^2 assuming $(\rho_s - \rho)$ = 1800 kg/m^3 for basalt.

From these calculations and measurements, the discharge needed to move sediment within the canyon can be calculated from the empirical formula of Bathurst (*S5*):

$$Q = UA = a(gRS)^{1/2}\left(\frac{h}{k_s}\right)^b A, \qquad (2)$$

where U is the average flow velocity across a channel cross section, A is the cross sectional area of flow, h is the average flow depth, and k_s is the roughness length scale of the bed. a and b were found empirically from measurements in mountain streams to be a = 3.84 and b = 0.547 for S < 0.8%, and a = 3.1 and b = 0.93 for S > 0.8% (*S5*).

Bathurst (*S5*) suggested $k_s \approx D_{84}$, although this likely depends on the site-specific substrate (e.g., bed forms, particle-size distribution, particle angularity). Others have shown that k_s can be two or three times D_{84} (e.g., *S6*). Instead of assuming k_s, we calculated it from equation (2) for conditions in Box Canyon creek using our surveyed cross section, water surface profile, and the USGS measured discharge (Q = 9.15 m^3/s) from March 2004 (*S7*). A cross section (XS2, Fig. 3) within the measurement reach was surveyed using a self leveling level and stadia rod (Fig. S4A). At the time of the

measurements, the maximum flow depth was 1.08 m and the average depth over the cross section was h = 0.58 m, which is equivalent to a hydraulic radius of R = 0.57 m. Within the measurement reach, the water surface slope at the time of our measurements was approximately uniform and equal to 0.9% (Profile P3, Fig. S3). Inserting these values into equation (2) results in k_s = 0.81 m, which is about one-third larger than our measured D_{84} within the reach. In the following calculations we use k_s = 0.81 m rather than D_{84} making our discharge estimates conservative.

At incipient motion, the hydraulic radius was calculated from equation (1) to be R = 1.6 m. Such a flow would fill the canyon at XS2 to an average depth of h = 1.7 m and a maximum depth of 2.5 m (Fig. S4A). Using these values and S = 1.85%, equation (2) was solved to find that a discharge $Q > 220$ m^3/s is needed to begin to move the sediment bed and continue canyon erosion.

Discharge of the flood event

The scoured channel upstream of the canyon head was used to estimate the discharge of the flood event. Aside from scour marks and a few plucked blocks along bedding planes, most of the bedrock surface within the channel is continuous with the neighboring land surface and appears to be the original volcanic surface. This suggests that the broad channel was not created by the flood event, but rather was inherited topography that likely focused flow towards the canyon.

A cross section (XS1, Fig. 3) was extracted from the LiDAR DEM (Fig. S4B), and at the threshold of overspill of the southern bank (which corresponds to a distance of ~ 25 m on Fig. S4B) was found have an area of 475 m^2. The water-surface slope during

the flood was assumed to be similar to the regional bedrock slope in the direction parallel to the scour marks (S = 0.74%), which was also extracted from the DEM. These measurements were used, along with a spectrum of roughness-length scales ($0.1 \le k_s \le 1$ m) to solve equation (2), resulting in a flow discharge ranging from 800 to 2800 m^3/s. Using the same parameters for the incipient-motion calculation above (i.e., S = 1.85% and k_s = 0.81 m), we found that this flood event would have filled the canyon to a depth ranging from 3.7 m to 5.8 m within our measurement reach (Fig. S4C).

Time to excavate the canyon

If sediment transport was the rate limiting step for canyon erosion, a duration of flow needed to carve the canyon can be estimated by dividing the total volume of the canyon (V) by a volumetric transport rate of sediment (Q_s). The total volume of the canyon (V = 1.53 x 10^7 m^3) was found using the DEM and differencing a surface interpolated from the topography surrounding the canyon and the topography of the canyon itself. For our estimated range of flood discharge (i.e., 800 - 2800 m^3/s) and the corresponding range in hydraulic radii (2.5 – 3.9 m), the volumetric transport rate was calculated as

$$Q_s = 5.7W\left(rgD_{50}^3\right)^{1/2}\left(\frac{\tau_b}{r\rho gD_{50}} - \tau_{*c}\right)^{3/2} \qquad (3)$$

where $r = (\rho_s - \rho)/\rho$ = 1.8 and W is the average bed-width of flow (*S8*), which at XS2 was found to be 47 m and 56 m for the two discharge estimates (Fig. S4C). This

calculation (i.e., V / Q_s) suggests that flow was sustained for 35 - 160 days to transport the required load out of the canyon.

^{4}He Cosmogenic exposure ages

The original up-direction and, if present, original lava-flow surface of the sampled boulders (e.g., Fig. S1B) was identified by basalt density (extent of vesicularity) and vesicle orientation. Samples were taken at least 1-m below volcanic-flow surfaces to avoid inherited exposure that resulted during hiatuses between basalt eruptions. In addition, the sample from the eroded notch was taken from ~2 m below the original flow surface as inferred by tracing bedding surfaces laterally. Helium exposure ages were measured on olivine separates from several kilograms of basalt taken from the upper 4 cm of the exposed surfaces. After extracting any magmatic helium from the olivine, cosmogenic ^{3}He was released from the samples by heating *in vacuo* and measured. Exposure ages were then calculated using an average production rate scaled for latitude, altitude and surface slope. The correction for shielding from canyon walls was found to be less than 4% for all samples and was folded into the error for each age determination. Measurements and calculations are further detailed in *(S9)*.

^{14}C Radiocarbon ages

The shells were extracted from a ~ 20-cm thick, finely laminated bed containing clay, silt and sand, which is exposed in a small road-cut within the talus slope (Fig. S1C). This bed is probably a backwater deposit from an unknown flood of the Snake River, and appears younger than the Yahoo Clay deposited throughout the region following

damming of the river by McKinny basalt flows (*S10*) ca. 52 ± 24 ka (*S11*), and older than the Bonneville flood (*S12*). Three dates from two shells within the layer yielded ^{14}C radiocarbon ages of 22.51 ± 0.07 ka, 22.55 ± 0.07 ka, and 22.34 ± 0.07 ka. The error bars represent two standard deviations. The first two dates are gas splits from acidification of the same shell. The measurements were made at the Keck Carbon Cycle AMS Facility, Earth System Science Department, University of California -Irvine, U.S.A, following the conventions of (*S13*). Sample preparation backgrounds were subtracted based on measurements of ^{14}C-free calcite.

Supporting Text

Geologic setting

Recently Gillerman et al. (*S14*) reinterpreted the basalt that composes Box Canyon as the Thousand Springs Basalt (also called Basalt of Flat Top Butte; ~ 395 ± 20 ka, (*S11*)), and the inferred the relatively young appearance of bedrock and the origin of Box Canyon to be from scour by the catastrophic Bonneville flood, which drained glacial lake Bonneville ca. 14.5 ka (*S12*). In his autobiography (*S15*), Stearns also admits the possibility that his seepage-erosion hypothesis (*S16*) was incorrect and that the Bonneville flood carved Box Canyon and scoured the neighboring landscape. Hydraulic modeling by O'Conner (*S17*), however, showed that the Bonneville flood did not overspill the Snake River Canyon in this region, which is consistent with our dating and analysis that Box Canyon was carved by an older event(s). U-Th/He eruption ages (*S9*) confirm that the basalt of Box Canyon is 86 ± 12 ka to 130 ± 12 ka and this is consistent

with the earlier designation of Sand Springs Basalt (*S18, S19*) (also named the Basalt of Rocky Butte (*S14*)) with an Ar-Ar eruption age of ~ 95 $\pm$ 10 ka (*S11*).

Near the mouth of Box Canyon, the Quaternary basalt overlies a ~ 5-m thick Pliocene or Miocene stratified volcaniclastic unit (*S14, S20*), which appears older and more weathered than the basalt. This unit is only exposed near the canyon mouth, where the talus slope was excavated recently for an aqueduct. Most of the canyon floor is composed of basalt boulders so the underlying bedrock cannot be determined. Quaternary basalt is exposed, however, at a ~5-m high waterfall (Fig. S5A) approximately 730 m downstream of the canyon head (Figs. 3 and S3). The log from the nearest well, about 0.5 km southeast of the canyon head, extends to a depth of 43 meters, or ~ 7 m below the canyon floor near the headwall, and indicates intact basalt to this depth (*S21*). Thus, if the underlying older unit is laterally extensive, it does not appear to have played a role in formation of the canyon, at least upstream of the waterfall.

Spring discharge and chemistry

Fig. S6 shows the daily average discharge and the dissolved silica concentration for Box Canyon creek as recorded by the U.S. Geological Survey (*S7*). The saturation value of 33 mg/L was calculated for dissolved quartz and amorphous silica at 14^{o} C and pH = 8 (*S22*), conditions typical of Box Canyon creek. Seasonal variations in discharge are less than 10 to 20% and trends over the 58-year duration of record are thought to record changes in farm irrigation across the plain, rather than natural forcing.

Talus at the canyon head

It is puzzling that there is almost no talus at the canyon head (Fig. S5B), while talus slopes are well developed elsewhere in the canyon. Our date of the notch at the canyon head suggests that wall collapse has not occurred there since ca. 45 ka. Perhaps, the basalt columns are more interlocked at the headwall, which might also explain why the headwall stalled at this location during canyon formation. Alternatively, maybe the spring flow prevents rock breakdown at the headwall, e.g. by preventing freeze-thaw (*S23*).

Delta at the canyon mouth

There appears to be a small delta (<<1% of the total canyon volume) at the mouth of Box Canyon (Fig. S5C). This might imply that there has been active transport of sediment since ca. 14.5 ka when the Bonneville flood swept through the Snake River Canyon (*S17*), or perhaps sediment transport occurred within Box Canyon because of withdrawal of the Bonneville floodwater.

Bedrock scour directions

Bedrock scours near the canyon head indicate flow towards the canyon headwall (Fig. 3). We identified three locations near the canyon mouth, however, with bedrock scours that appear to display an opposite flow direction with orientations ranging from 113 ^{o} to 115 ^{o} (Table S1). The consistency of these directions, all aligned with the prevailing westerly wind direction, suggests that these outliers resulted from wind abrasion. A high knob of bedrock ~ 7.8 km to the east of Box Canyon also shows scours orientated 110 ^{o} consistent with this hypothesis.

Supporting Figures

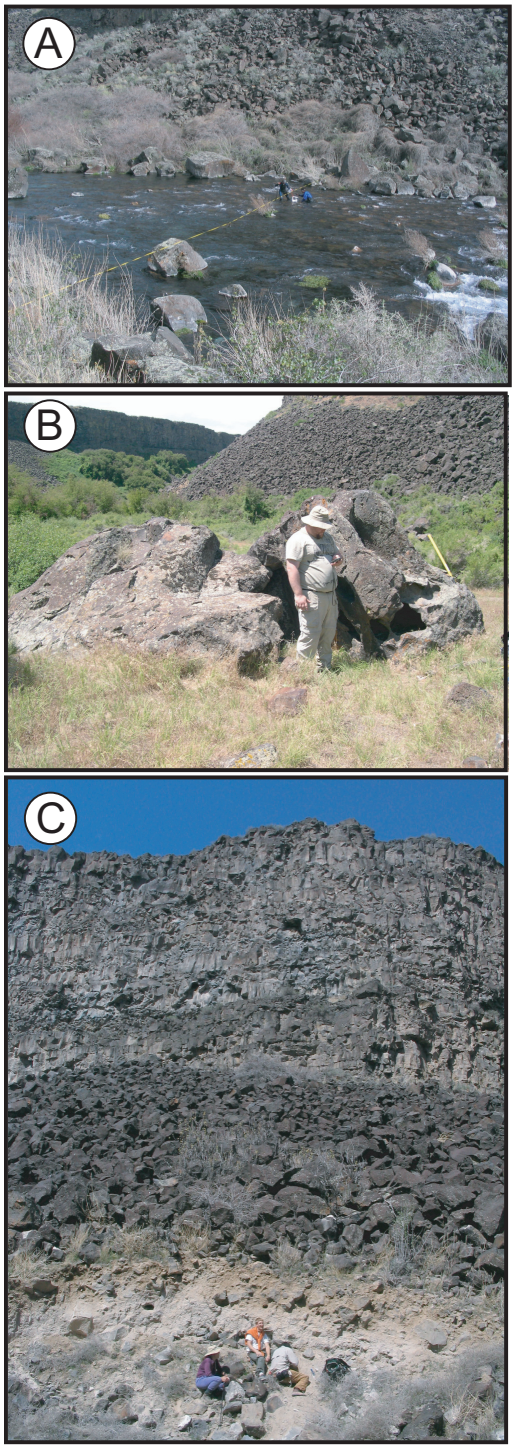

Fig. S1. (A) Photograph of the measurement reach and cross section XS2 within Box Canyon (the stream is ~ 35 m wide for scale). (B) Photograph of the boulder at location 2 (Fig. 3) sampled for ^{4}He cosmogenic exposure dating. (C) Photograph of a sediment deposit exposed within the talus slope (location 5, Fig. 3) containing shell fragments that were used for ^{14}C dating.

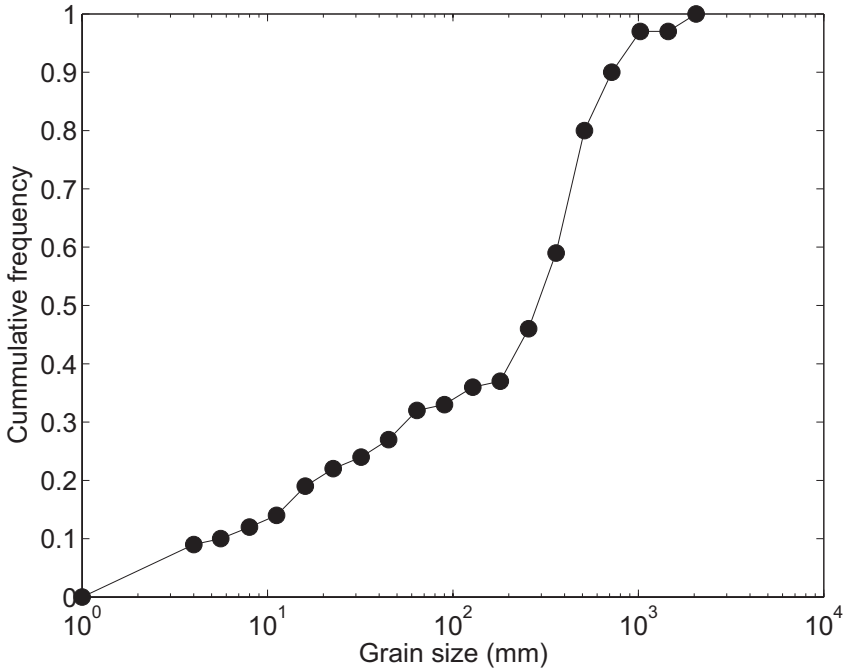

Fig. S2. Cumulative frequency distribution of particle sizes along the stream bed of Box Canyon within the measurement reach.

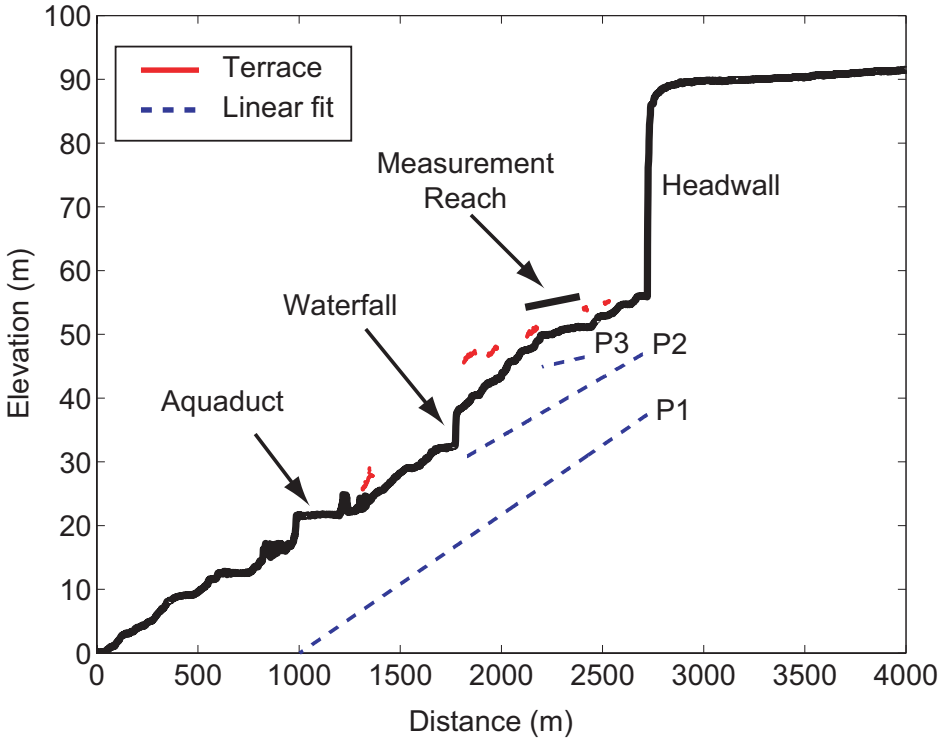

Fig. S3. Longitudinal profile of Box Canyon calculated as the path of steepest descent from the 1-m resolution DEM. Three linear, least-squares fits to the data, used to calculate channel-bed slope, are shown as dashed lines (displayed offset from the data) for P1: the entire length of the canyon (S = 2.18%), P2: a 900-m reach bounded by the waterfall and the canyon head (S = 1.85%), and P3: the measurement reach (S = 0.9%). The elevations of mapped terraces (Fig. 3) are shown in red.

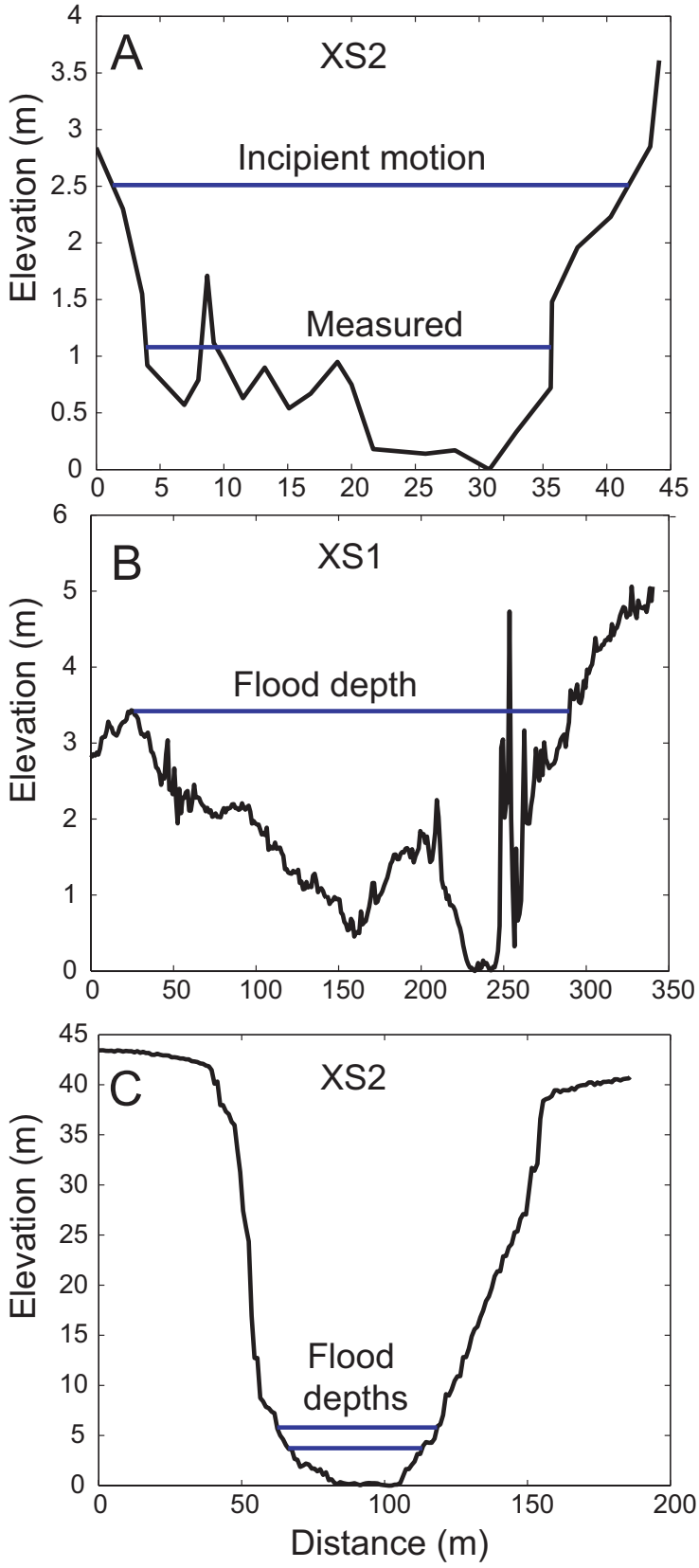

Fig. S4. Cross sections of Box Canyon. (A) XS2 (Fig. 3) along the stream bed showing the bed and water surface topography surveyed in the field, as well as the calculated depth for incipient motion. (B) XS1 (Fig. 3) extracted from the DEM showing the depth used to constrain the flood discharge. (C) XS2 extracted from the DEM showing a range in depths that correspond to the range in calculated flood discharges.

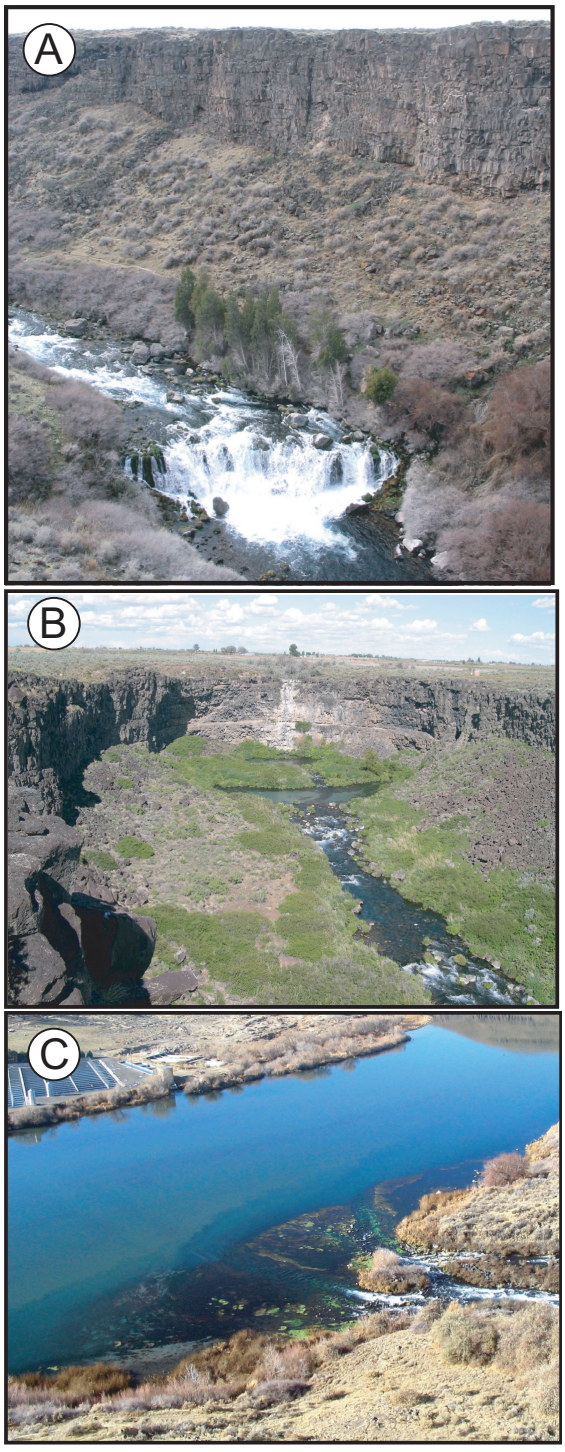

Fig. S5. Photographs of Box Canyon showing the (A) ~ 5-m high waterfall, (B) ~ 35-m high canyon headwall, and (C) small delta at the confluence with the Snake River (the Snake River is ~ 200 m wide for scale).

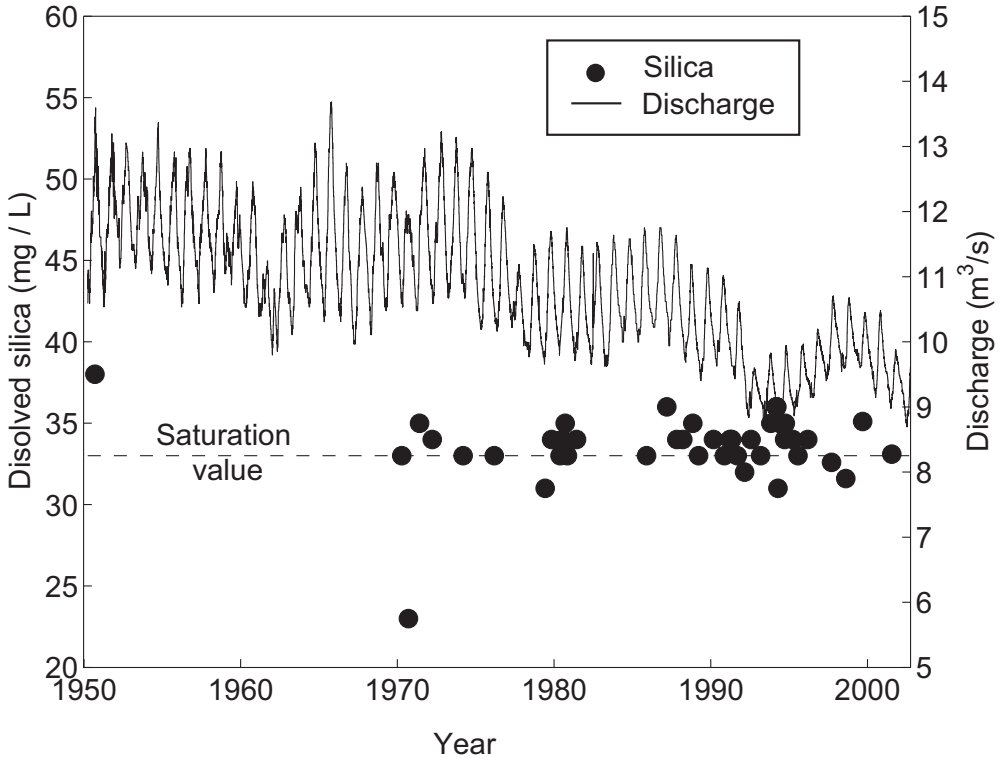

Fig. S6. Discharge and dissolved silica records for Box Canyon creek from the U.S. Geological Survey gauge 13095500.

Supporting Tables

Table S1 – Inferred wind abrasion marks.

Location	Longitude	Latitude	Scour orientation
Box Canyon	42.70566˚	-114.81971˚	113˚
Box Canyon	42.70902˚	-114.81895˚	115˚
Box Canyon	42.70874˚	-114.82214˚	115˚
7.8 km East	42.7163˚	-114.70708˚	110˚

Supporting References and Notes

S1. A. Shields, *Mitt. Preuss. Versuchsanst. Wasserbau Schiffbau* **26**, 26 (1936).

S2. J. M. Buffington, D. R. Montgomery, *Water Resources Research* **33**, 1993 (1997).

S3. D. R. Montgomery, J. M. Buffington, *Geological Society of America Bulletin* **109**, 596 (1997).

S4. M. P. Lamb, W. E. Dietrich, J. Venditti, *Journal of Geophysical Research* in press, (available at http://www.agu.org/journals/pip/jf/2007JF000831-pip.pdf).

S5. J. C. Bathurst, *Journal of Hydrology* **269**, 11 (2002).

S6. J. W. Kamphuis, *Journal of Hydraulic Research* **12**, 193 (1974).

S7. U.S. Geological Survey, gauge 13095500, Box Canyon Creek, Idaho

S8. R. Fernandez Luque, R. van Beek, *J. Hydraul. Res.* **14**, 127 (1976).

S9. S. M. Aciego *et al.*, *Earth and Planetary Science Letters* **254**, 288, doi:10.1016/j.epsl.2006.11.039 (2007).

S10. H. E. Malde, in *Cenozoic Geology of Idaho* B. Bonnichsen, R. M. Breckenridge, Eds. (1982), vol. 26, pp. 617-628.

S11. L. Tauxe, C. Luskin, P. Selkin, P. Gans, A. Calvert, *Geochemistry Geophysics Geosystems* **5**, doi:10.1029/2003GC000661 (2004).

S12. W. E. Scott, K. L. Pierce, J. P. Bradbury, R. M. Forester, in *Cenezoic Geology of Idaho: Idaho Bureau of Mines and Geology Bulletin* G. Bonnichsen, R. M. Breckenridge, Eds. (1982), vol. 26, pp. 581-595.

S13. M. Stuiver, H. A. Polach, *Radiocarbon* **19**, 355 (1977).

S14. V. S. Gillerman, J. D. Kauffman, K. L. Otherberg, *Geologic map of the Thousand Springs Quadrangle, Gooding and Twin Falls counties, Idaho* (Idaho Geological Survey, Moscow, Idaho, 2004).

S15. H. T. Stearns, *Journal of Geology* **44**, 429 (1936).

S16. H. T. Stearns, *Memoirs of a Geologist: From Poverty Peak to Piggery Gulch* (Hawaii Institute of Geophysics, Honolulu, Hawaii, 1983).

S17. J. E. O'Connor, *Hydrology, Hydraulics and Geomorphology of the Bonneville Flood*, GSA Special Paper 274 (Geological Society of America, Boulder, CO, 1993), pp. 90.

S18. H. E. Malde, *U.S. Geological Survey Professional Paper*, 20 (1971).

S19. H. R. Covington, J. N. Weaver, *Geologic map and profiles of the north wall of the Snake River Canyon, Thousand Springs and Niagara Springs quadrangles, Idaho*, U.S. Geological Survey Miscellaneous Investigations I-1947C (1991).

S20. H. E. Malde, H. A. Powers, *Geological Society of America Bulletin* **73**, 1197 (1962).

S21. Elsing Well Drilling, Well Log # 40916, Department of Water Resources, Idaho (1975).

S22. G. Faure, *Principles and Applications of Geochemstry* (Prentice Hall, Upper Sadle River, ed. 2nd, 1998), pp. 600.

S23. L. J. Mason, D. T. Pederson, R. J. Goble, *Eos Trans. AGU Fall Meet. Suppl.* **85**, Abstract H51C (2004).